ENDOR and ESR Studies of Radical Cations of Methyl-Substituted Benzene in Halocarbon Matrices

R. M. Kadam, Y. Itagaki, R. Erickson, and A. Lund*

Department of Physics and Measurement Technology, Linköping University, S-58183 Linköping, Sweden

Received: November 2, 1998; In Final Form: January 16, 1999

The radical cations of methyl-substituted benzene toluene, *p*-xylene, *o*-xylene, *m*-xylene, and their deuterated analogues generated in $CFCl_3$ and CF_3CCl_3 matrices by X-ray irradiation at 77 K were investigated by ESR and high-resolution ENDOR spectroscopy. The ESR and ENDOR spectra in these radical cations are dominated by large axially symmetric hyperfine splitting due to methyl-group protons. The anisotropic hyperfine coupling constants (hfcc) of methyl protons and ring protons in radical cations of toluene and *p*-xylene were measured accurately by ENDOR spectroscopy. In the case of deuterated *p*-xylene and *o*-xylene radical cations in CF_3-CCl_3 matrix, the hyperfine coupling constants are scaled by their magnetogyric ratio ($\gamma_H/\gamma_D = 6.51$). Theoretical calculations of the isotropic and dipolar hyperfine coupling constants in these radical cations are found to be in good agreement with experimental results. The experimental and theoretical calculations supported the stabilization of the $^2B_{2g}$ type of state for the radical cations of toluene and *p*-xylene compared to the stabilization of the $^2B_{1g}$ type of ground state for *o*-xylene and *m*-xylene due to lifting of the orbital degeneracy of the e_{1g} orbital by lowering the symmetry obtained after substitution of hydrogen by methyl group.

1. Introduction

In contrast to many radical cations of aromatic hydrocarbons, the radical cations benzene, toluene, and xylenes are difficult to stabilize and study in solutions. However, these radical cations can be prepared in glassy rigid matrices of certain halocarbons or on surfaces of zeolite or silica gel.[1−11] The benzene cation is of fundamental interest because it possesses an orbitally degenerated ground state e_{1g} (D_{6h}) and is subjected to a Jahn−Teller distortion at low temperature.[6,12] The substitution of hydrogen by weakly perturbing alkyl groups, like the methyl group in toluene and xylene anions, removes the 2-fold orbital degeneracy of the ground state of benzene radical cations/anions artificially.[13,14] The radical cations of toluene and xylene in silica gel and halocarbon matrices have been reported previously.[15−17] The hyperfine coupling constants determined in these investigations were different and a detailed assignment of the spectra is still lacking. Komatsu et al.[18] studied the radical cations of toluene and partly deuterated toluene (toluene α-d_3) on silica gel and Vycor glass and gave unambiguous evidence for the formation of toluene radical cation.

ESR is used for providing information of the spin density distribution. ESR also reveals the symmetry of the SOMO, which reflects the HOMO and LUMO of the mother molecule in the case of radical cations and anions, respectively. The ESR spectra of radical cations in glassy matrices suffer from limited spectral resolution as they are usually broad when compared to spectra of radical cations adsorbed on molecular sieve/zeolites. Furthermore, in glassy/disordered matrices the ESR spectral resolution is reduced due to *g* and hyperfine anisotropy, and inhomogeneous line broadening. Also, interaction of the unpaired electron with more than one type of inequivalant nuclei increases the number of ESR transitions. This can make an interpretation of the spectra difficult. In the present study, the ESR spectra of radical cations of methyl-substituted benzene is dominated by the methyl-proton splitting and it is often difficult to make an unambiguous assignment to the smaller hyperfine coupling constants arising from ring protons. Therefore, we have used a high-resolution electron nuclear double resonance (ENDOR) technique for estimating anisotropic hyperfine coupling parameters with higher precision. For benzene, biphenyl, and naphthalene radical cations the higher resolution of ENDOR spectroscopy has greatly facilitated investigations of the anisotropic ring proton hyperfine tensors in disordered solids.[8−10] However, powder ENDOR spectra are often not as straightforward to interpret as spectra in solutions and single crystals. Although anisotropy of hyperfine and quadrupolar interactions can produce complex line shapes in a powder ENDOR spectrum, computer simulations of the spectrum can greatly aid an accurate assignment of spectroscopic parameters.

In the present paper we describe our ESR and ENDOR results on radical cations of methyl-substituted benzene in $CFCl_3$ and CF_3CCl_3 matrices. From the ENDOR measurements we have accurately measured the hyperfine tensor anisotropy for methyl and ring protons in the case of toluene and *p*-xylene. The geometries, isotropic ^1H hfc and π-electron spin densities of radical cations of methyl-substituted benzene, which were theoretically evaluated by DFT (density functional theory) calculations supported the experimental results. The experimental and theoretical calculations supported the stabilization of the $^2B_{2g}$ type of state for radical cations of toluene and *p*-xylene compared to the stabilization of the $^2B_{1g}$ type of ground state for *o*-xylene and *m*-xylene due to lifting of the orbital degeneracy of the e_{1g} orbital.

2. Experimental Section

The chemicals used in the present study were toluene, *p*-xylene, *o*-xylene, *m*-xylene, fully deuterated *p*-xylene and

* To whom the correspondence should be addressed. E-mail: alund@ifm.liu.se. Tel: +46 13 28 2665. Fax: +46 13 13 7568.

10.1021/jp9843149 CCC: $18.00
Published on Web 03/03/1999

o-xylene, $CFCl_3$, and CF_3CCl_3, obtained commercially, and these were used without further purification. Solid solutions of 1 mol % of solute in $CFCl_3$ and CF_3CCl_3 matrices were prepared in quartz tubes after degassing on a vacuum line (less than 10^{-4} Torr). The radical cations of methyl-substituted benzenes in these matrices were generated by irradiating the samples for 10 min at 77 K using an X-ray source with a tungsten anode operating at 50 kV and 50 mA. ESR and ENDOR spectra were recorded on a Bruker ER200 spectrometer with an ENDOR attachment. The radio frequency field was amplified using a 100 W ENI amplifier. The temperature was varied in the range 100−150 K using a Bruker VT 4111 variable-temperature controller.

3. Theoretical Calculations

All calculations were carried out by using the Gaussian 94[19] program package on the Cray computer at IFM, Linköping University. The optimized structures and spin densities for toluene, *o*-, *m*- and *p*-xylene radical cations were obtained by employing several DFT (density functional theory) methods with a 6-31++G(d,p) basis set with polarization and diffusion functions. The density functionals employed in the present work were BLYP, B3LYP, BVWN, and BVWN5, where BLYP is a Becke 88 exchange along with the Lee−Yang−Parr (LYP) correlation, B3LYP is Becke's three-parameter exchange correlation and LYP correlation, and BVWN and BVWN5 are Becke's exchange with Vosko, Wilk, and Nusair 1980 correlation functionals. The isotropic hyperfine coupling constants were evaluated from a Fermi contact analysis in DFT methods. Anisotropic hyperfine couplings were obtained using DFT-optimized geometries and INDO spin densities. The value 3.102 was selected as effective nuclear charge for carbon atoms introduced by Edlund and co-workers.[20]

4. Experimental Results

The aromatic radical cations in the $CFCl_3$ matrix have a tendency to form partly oriented samples in which the amount of order/disorder depends on the concentration of the solute and freezing rate.[12] We have made sure the polycrystalline nature of these samples by rotating the sample in the static magnetic field. No orientational dependence in line shape was observed, indicating a truly polycrystalline nature, whereas the aromatic radical cations in CF_3CCl_3 matrix only form glassy samples.

4.1. ESR and ENDOR Results. *(i) ESR of Toluene Radical Cations in CF_3CCl_3 and $CFCl_3$ Matrices.* The radical cations of toluene have previously been observed by ionization of neutral species in Freon,[16,17] on silica gel and HY matrices.[15,18] X-ray irradiated toluene (1 mol %) in $CFCl_3$ and CF_3CCl_3 matrices at 120 K gave a sextet hyperfine structure in its ESR spectrum ($a_{CH3} = 2.0$ mT, $a_{H4} = 1.0$ mT), as shown in Figure 1. The ESR line shape is mainly caused by pronounced hyperfine anisotropy of the ring proton at a para position and small but definite hyperfine anisotropy of the methyl group. The weaker hyperfine interaction of the H_2 and H_6 protons contributes to the line width of the ESR spectrum. Higher content of toluene (nearly 10 mol %) in the CF_3CCl_3 matrix could stabilize dimeric radical cations of toluene (with the hyperfine coupling nearly half to that of toluene monomers) and will not be discussed further in this work.

(ii) ENDOR Results, Simulation, and Line Assignments. The experimental ENDOR spectra of toluene radical cations in the $CFCl_3$ and CF_3CCl_3 matrices at 120 K are presented in Figure 2. These spectra were obtained by sweeping the radio frequency between 1 and 51 MHz and by pumping at the magnetic field of the central ESR signal. The best resolved ENDOR spectrum was obtained from the CF_3CCl_3 sample showing sharp lines from both ring and methyl protons. The ENDOR signal in the region of 14 MHz is complicated as it contains a small contribution from a radical signal generated from the matrix in addition to the signal from the radical cation. Transitions outside

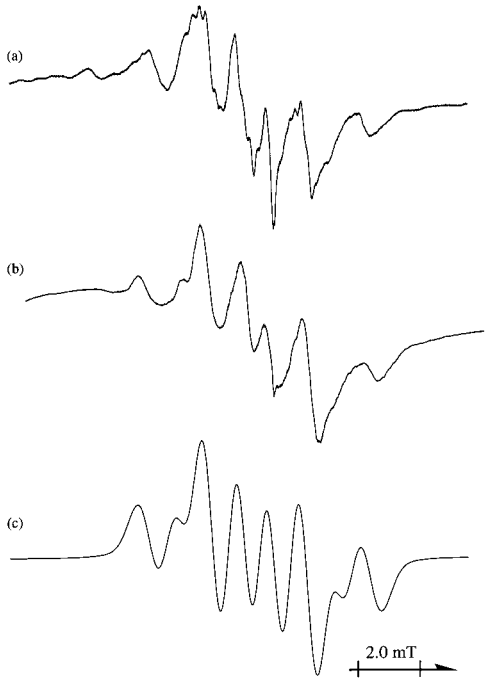

Figure 1. ESR spectra of the radical cation of toluene in (a) $CFCl_3$ and (b) CF_3CCl_3 matrices measured at 120 K after X irradiation at 77 K. (c) Simulated spectrum obtained by using the parameters shown in Table 1.

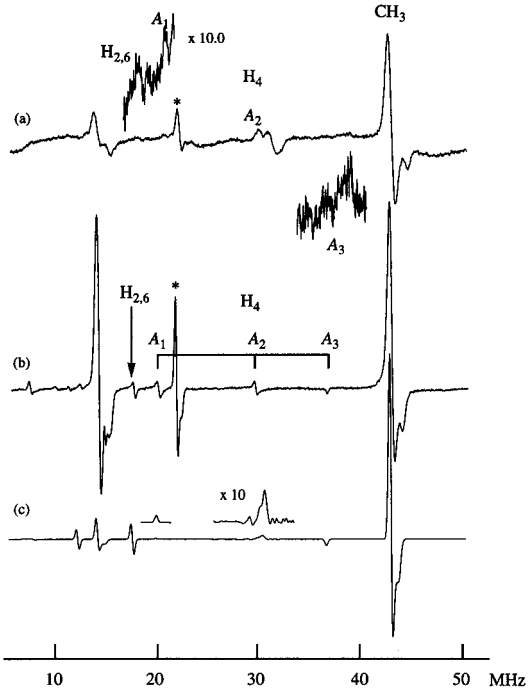

Figure 2. ENDOR spectra of the radical cation of toluene in (a) $CFCl_3$ and (b) CF_3CCl_3 matrices measured at 120 K after X irradiation at 77 K. (c) Simulated spectrum obtained by using the parameters in Table 1.

this region are caused by intensity buildup corresponding to principal values of the ring proton hyperfine tensor. The ENDOR transitions are symmetrically placed around the proton Larmor frequency, near $\nu_H \pm A_i/2$ MHz. The line at 43 MHz, with a pairing line at 14.00 MHz, corresponds to methyl protons. The hyperfine tensor of the methyl protons is nearly axially symmetric. For para proton, lines from all principal directions, i.e., the lines at 37, 30, and 20 MHz with their pairing lines in the low-frequency region, are observed. The hyperfine tensor of the para proton is expected to be of α-proton type with three principal components close to 1.5*a*, *a*, 0.5*a* that are perpendicular to the C−H bond, normal to the benzene ring and along the C−H bond (*a* is the isotropic hyperfine coupling). The proton at the ortho position has small hyperfine tensor components, and lines observed in the 17.5 MHz region could be attributed to them. It should be noted that in Figure 2, lines marked with an asterisk at 21.99 MHz are the second harmonics of the strongest ENDOR lines due to the nonlinearity of the radio frequency power amplifier. As can be seen in Figure 2, the transitions below ν_H have lower intensity than the pairing lines above, as explained in terms of a so-called hyperfine enhancement effect reported by several authors.[21−23] The simulation also predicts them to have a very low intensity. The radical cation of toluene in the $CFCl_3$ matrix showed a pronounced axially symmetric ENDOR signal arising from the methyl group, and a set of relatively weaker signals with large hyperfine anisotropy arising from the proton at para position. There are small differences in the principal values of the hyperfine coupling constants between these two samples presumably due to the matrix effect. The hyperfine coupling constants obtained from the ENDOR measurements for the radical cations of toluene and *p*-xylene are given in Table 1. The ESR and ENDOR spectra could be simulated accurately using the hyperfine coupling constants given in Table 1. The dipolar hyperfine coupling constants obtained from the ENDOR measurements are listed in Table 2 along with the estimates obtained from theoretical calculations.

(iii) ESR of p-Xylene and Deuterated p-Xylene (d_{10}) Radical Cations in $CFCl_3$ and CF_3CCl_3 Matrices. The ESR spectra of *p*-xylene radical cations in $CFCl_3$ and CF_3CCl_3 matrices at 120 K consist of a well-resolved septet of quintets ($a_{CH3} = 1.9$ mT, $a_{H2,3,5,6} = 0.45$ mT). The ESR spectrum of deuterated *p*-xylene radical cations in a CF_3CCl_3 matrix showed 13 lines as expected from intensity distribution from two equivalent $-CD_3$ groups ($a_{iso} = 0.29$ mT) as shown in Figure 3. The hyperfine splitting from ring deuteriums (2, 3, 5, and 6 position) in this radical cation is not resolved in the ESR spectra. The hyperfine splittings in deuterated *p*-xylene is reduced by the magnetogyric ratio ($\gamma_H/\gamma_D = 6.51$).

(iv) ENDOR Results, Simulation, and Line Assignments. Well-resolved ENDOR spectra of the *p*-xylene radical cation in halocarbon matrices at 120 K were obtained and they showed two sets of ENDOR transitions. The first set at 41 MHz with its pairing line at 12 MHz is due to methyl groups (axially symmetric) and the second set (19, 20.9, and 21.5 MHz) with a relatively small hyperfine anisotropy is due to ring protons, Figure 4a. The corresponding pairing lines at the low-frequency side are 9 and 11 MHz. We have considered the small hyperfine anisotropy of ring protons as observed in the ENDOR spectrum in order to obtain more faithful simulation of the ESR spectrum. Theoretical calculations confirmed hyperfine anisotropy for ring protons. The ENDOR spectrum of deuterated *p*-xylene radical cations in CF_3CCl_3 matrix showed a complicated pattern involving some extra lines in the region 4−6 MHz as shown in Figure 4c. These lines should be attributed to the matrix signal since no hyperfine couplings from radical cations of deuterated *p*-xylene are expected in this range. By comparing the hyperfine couplings with those of the undeuterated sample, the ENDOR transitions in the deuterated *p*-xylene radical cations at 7 MHz with its pairing line at 2.4 MHz was assigned to the $-CD_3$ group and another cation at 3.73 MHz to ring deuteriums. It may be noted that the hyperfine anisotropy arising from ring deuteriums is not resolved as in the case of undeuterated sample. The simulated ESR and ENDOR spectra of *p*-xylene radical cations are shown in Figures 3 and 4, respectively.

(v) ESR and ENDOR Results of o-Xylene and m-Xylene Radical Cations in CF_3CCl_3 and $CFCl_3$ Matrices. The ESR

TABLE 1: Experimental *g* and Hyperfine Tensors (in MHz) Obtained for a Series of Methyl-Substituted Benzene Radical Cations in CF_3CCl_3 and $CFCl_3$ (in Parentheses) Matrices at 120 K[a]

compounds	principal components	principal values (MHz)	direction cosines		
			x	*y*	*z*
toluene$^+$	g_{iso}	2.0029			
A_{CH3}	A_x	+56.34 (+55.24)	1	0	0
	A_y	+58.38 (+55.24)	0	1	0
	A_z	+56.34 (+58.80)	0	0	1
	a_{iso}	+57.00 (+56.43)			
A_{H4}	A_x	−43.75 (−48.50)	1	0	0
	A_y	−10.00 (−10.00)	0	1	0
	A_z	−28.50 (−32.06)	0	0	1
	a_{iso}	−27.42 (−30.19)			
$A_{H2,6}$	a_{iso}	−5.40 (−5.40)			
p-xylene$^+$	g_{iso}	2.0029			
A_{CH3}	A_x	+52.00	1	0	0
	A_y	+55.25	0	1	0
	A_z	+52.00	0	0	1
$A_{H2,3,5,6}$	a_{iso}	+53.08 (+51.63)			
	A_x	−12.50	±0.3771	0.9262	0
	A_y	−7.00	−0.9262	±0.3771	0
	A_z	−11.92	0	0	1
	a_{iso}	−10.47 (−9.04)			
o-xylene$^+$	g_{iso}	2.0029			
A_{CH3}	A_x	(+37.41)			
	A_y	(+37.41)			
	A_z	(+40.85)			
	a_{iso}	(+37.36)			
$A_{H4,5}$	a_{iso}	(−15.53)			
m-xylene$^+$	g_{iso}	2.0029			
A_{CH3}	A_x	34			
	A_y	34			
	A_z	36			
	a_{iso}	34.67			

[a] Conversion factor is 1 G = 2.8025 g/g_e MHz.

TABLE 2: Experimental and Theoretical Dipolar Hyperfine Tensors (in MHz) for a Series of Methyl-Substituted Benzene Radical Cations in CF_3CCl_3 and $CFCl_3$ (in parentheses) Matrices at 120 K

compounds	principal components	exptl values (MHz)	theoretical values (MHz)
toluene$^+$			
A_{H4}	B_x	−16.35 (−18.31)	−16.85
	B_y	+17.42 (+20.19)	+20.01
	B_z	−1.09 (−1.88)	−3.130
p-xylene$^+$			
$A_{H2,3,5,6}$	B_x	−2.02	−3.166
	B_y	+3.47	+5.628
	B_z	−1.46	−2.462
benzene$^+$			
$A_{H1,4}$	B_x	−13.50[6]	−16.0[25]
	B_y	+14.22	+18.8
	B_z	−0.70	−2.8

[a] Conversion factor is 1 G = 2.8025 g/g_e MHz.

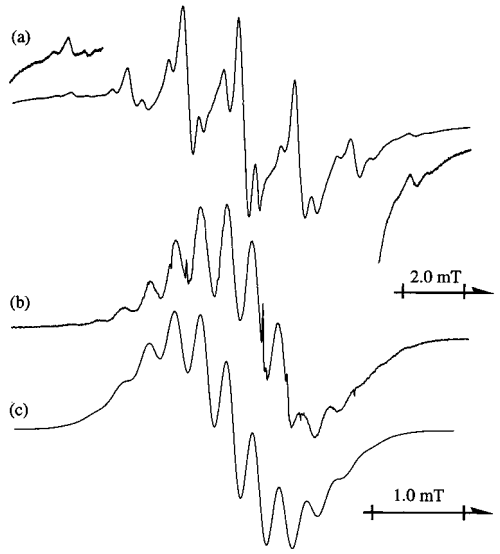

Figure 3. ESR spectra of the radical cation (a) *p*-xylene and (b) a completely deuterated analogue (-d_{10}) in a CF_3CCl_3 matrix measured at 120 K after X irradiation at 77 K. (c) Simulated spectrum obtained for completely deuterated *p*-xylene obtained by using the parameters in Table 1 scaled by the magnetogyric ratio (γ_H/γ_D).

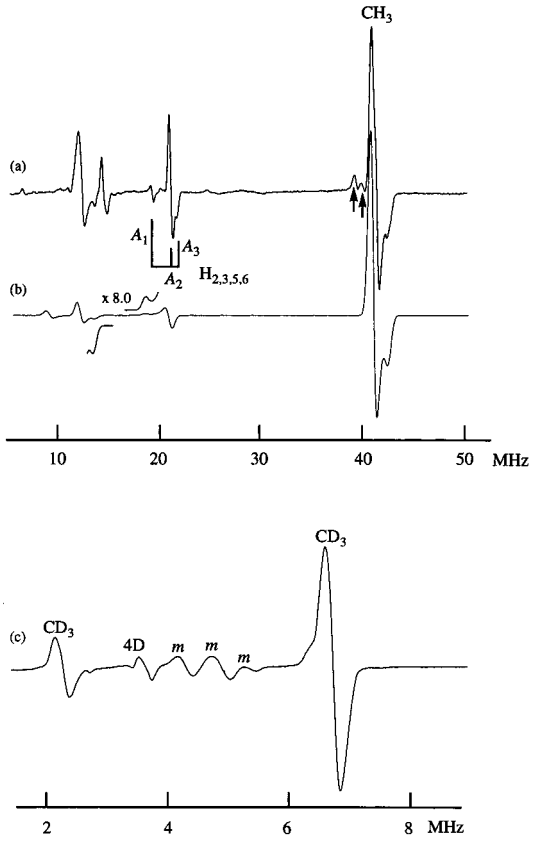

Figure 4. ENDOR spectra of the radical cation (a) *p*-xylene and (c) a completely deuterated analogue (-d_{10}) in a CF_3CCl_3 matrix measured at 120 K after X irradiation at 77 K. The signals marked by arrows and "*m*" are due to contribution from small concentration of anther sites and matrix radical, respectively. (b) ENDOR simulation for *p*-xylene.

spectrum of radical cations of *o*-xylene and *m*-xylene in CF_3CCl_3 matrix gave methyl-proton hyperfine splittings of 1.3 and

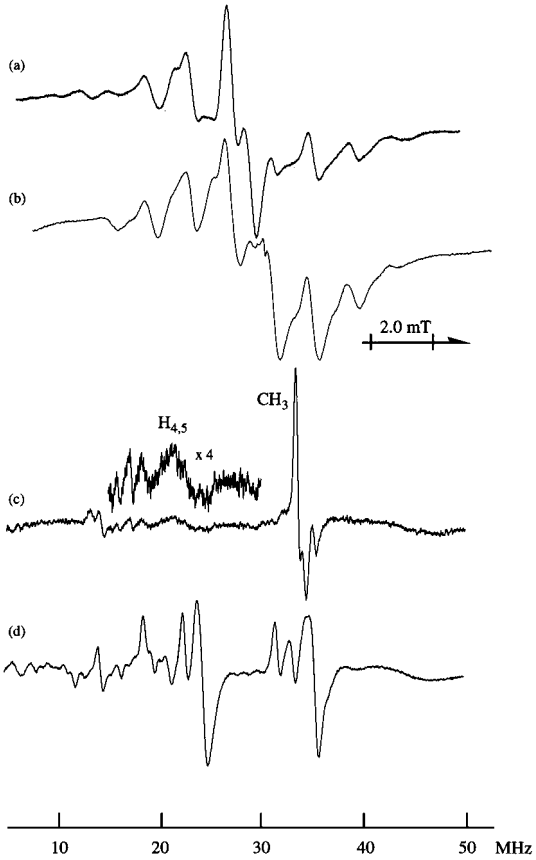

Figure 5. ESR and ENDOR spectra of the radical cation of *o*-xylene in $CFCl_3$ and CF_3CCl_3 matrices measured at 120 K after X irradiation at 77 K. ESR spectra in $CFCl_3$ and CF_3CCl_3 are shown in (a) and (b), and the corresponding ENDOR spectra are shown in (c) and (d).

1.2 mT, respectively. These splittings are quite close to those reported earlier.[16,17] The ENDOR spectrum of *o*-xylene and *m*-xylene in a CF_3CCl_3 matrix showed a number of ENDOR transitions in the high-frequency region (15−35 MHz). This is probably due to stabilization of different sites for these radical cations which have very small differences in their principal hyperfine coupling tensors. It is also due to the hyperfine anisotropy arising from ring protons. These different sites are difficult to identify in ESR spectra due to low resolution. The hyperfine coupling constants for radical cations of *o*-xylene in $CFCl_3$ matrix are extracted from the ENDOR spectra which exhibit a relatively simple patterns having intense transitions near 33.70 MHz and a broad transition at 23.96 MHz (A_{CH3} = 1.35 mT and $A_{H3,4}$ = 0.64 mT). The ESR spectrum of deuterated *o*-xylene radical cations in a CF_3CCl_3 matrix is only a single broad line at 120 K, whereas the ENDOR spectrum consists of two strong signals which are assigned to couplings with $-CD_3$, D_3, and D_4 nuclei. This spectrum is not shown in the figure. The ESR and ENDOR results of *o*-xylene and *m*-xylene radical cations in halocarbon matrices are presented in Figures 5 and 6. We have not attempted the simulations of the ESR spectrum of these radical cations because it is evident from its ENDOR spectra that simultaneous stabilization of different sites with different concentrations occurs.

4.2. Calculation Results. *(i) Optimized Structures.* All optimized structures of toluene and *o*-, *m*-, and *p*-xylene radical cations obtained in the present study were found to be planar in which one of the methyl protons is lying in the benzene ring plane. The computations suggest that geometrical deformations took place by one-electron oxidation, or ionization. Hasegawa and co-workers[24] have reported that geometrical deformations

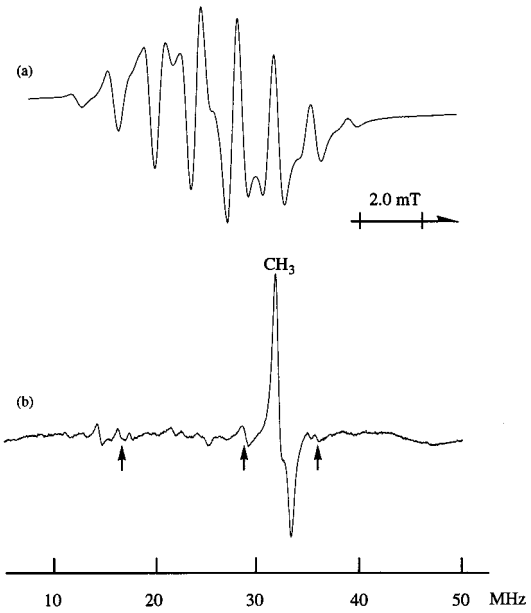

Figure 6. (a) ESR and (b) ENDOR spectra of the radical cation of *m*-xylene in CF_3CCl_3 matrices measured at 120 K after X irradiation at 77 K. The signals shown by arrows are expected anisotropic hyperfine transitions due to ring protons (H_4 and H_6) obtained from the INDO calculations.

CHART 1: Schematic Representation for the Jahn−Teller Distortion of the Benzene Radical Cation[a]

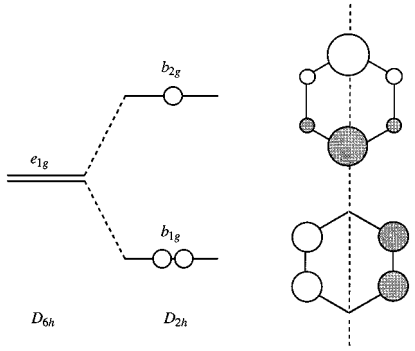

[a] The dotted line is a C_2 axis. The ring elongation and compression occur along this direction.

from the neutral mother molecules take place for a series of fluorinated benzene radical cations. They concluded that fluorinated benzene cations can be classified into two groups in terms of the deformations. One is the ring elongation in the direction of a molecular axis, shown as a dotted line in Chart 1, and the other group is ring compression in the same direction. Interestingly, mono, 1,2-, 1,3-, and 1,4-methylbenzene cations and the corresponding fluorobenzene cations belong to the same groups. It is well-known that both methyl groups and fluorine have a positive inductive effect that induces electron repulsion through the π-bond between the ring carbon and the methyl group carbon or the fluorine. This is expected to be the main factor for removing the orbital degeneracy leading the α-carbons to acquire large spin densities.

The bond lengths and bond angles of methyl-substituted benzene radical cations as evaluated by the B3LYP method are shown in Figure 7 along with the deviation from the corresponding neutral mother molecules. In the case of the radical cation of toluene and *p*-xylene, ring compression was suggested, whereas in the case of *o*- and *m*-xylene radical cations ring elongation along the *y* direction was suggested (see Figure 7).

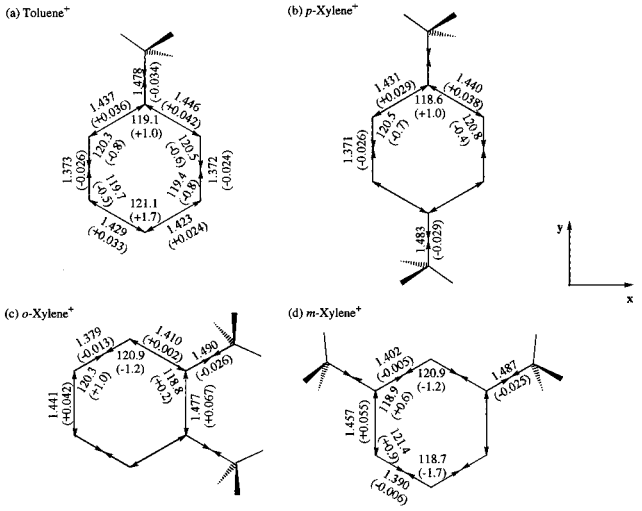

Figure 7. Optimized geometries of the radical cations of a series of methyl-substituted benzenes obtained by using B3LYP/6-31++G** level of theory. The bond lengths in angstroms and angles in degrees are given together with the difference from the corresponding optimized geometries of the neutral molecules (in parentheses).

In the process of ionization, or electron releasing from the HOMO, chemical bonds with bonding features are elongated and those with antibonding features are compressed. Toluene and *p*-xylene cations have four elongated bonds (C_1-C_2, C_1-C_6, C_3-C_4, and C_4-C_5) and two compressed bonds (C_2-C_3 and C_5-C_6). The *o*- and *m*-xylene cations have two elongated bonds, and the remaining four bonds have almost the same lengths as their mother molecules. Therefore, from the optimized geometrical structures, taking only the ring carbons into account, we suggest that the unpaired electron in the case of toluene and *p*-xylene cations has a $^2B_{2g}$ character as has been reported for the benzene radical cation[12] in a $CFCl_3$ matrix in contrast to a $^2B_{1g}$ ground state for the *o*- and *m*-xylene cations in halocarbon matrices.

The spin expectation values of S^2 {$=s(s+1)$} in all calculations were in a range from 0.7538 to 0.7618, implying quite small spin contamination.

(ii) Spin Density Distribution and ^1H Hf.[5] The theoretical spin densities estimated for the α-carbons which are bonded to the methyl group are reduced in the following order, toluene > *p*-xylene > *m*-xylene > *o*-xylene. This is in accordance with the trend in the proton hyperfine coupling for the methyl group. As regards the toluene cation, the spin density on the para carbon (C_4) is slightly larger than that on the α-carbon C_1 (0.363 for C_4 and 0.321 for C_1 in the result of the BLYP calculation; see Table 3). In fact the isotropic hyperfine coupling of the para proton in the toluene cation (27.42 MHz in CF_3CCl_3 and 30.19 MHz in $CFCl_3$) is larger than that for the protons at 1 and 4 position in the $^2B_{2g}$ benzene cations caused by Jahn−Teller distortion (23.0 MHz[12]). The spin density distribution at C_2 and C_6 is much larger than that at C_3 and C_5 (0.087 for the former carbons and 0.017 for the latter ones in the BLYP calculation). Note that the spin densities on the carbons in Table 3 are shown as averaged values among the symmetric carbons taking free rotation of the methyl group into account. INDO calculation for the radical cation of toluene has been carried out by Chandra and co-workers.[26] Although the isotropic hyperfine coupling for the methyl protons in their case was overestimated, the trend of the spin density distribution was the same as in our results. The two equivalent C_1 and C_4 carbons in the *p*-xylene cation

TABLE 3: Theoretical Isotropic Hf (in MHz) and π-Electron Spin Densities[a] of Methyl-Substituted Benzene Radical Cations Together with Experimental Values

		density functionals				
		BLYP	B3LYP	BVWN	BVWN5	experiment[c]
toluene$^+$						
^{1}H-hf	CH_3	67.09	60.82	59.47	59.44	57.00 (56.43)
	$H_{2,6}$	−7.756	−8.120	−7.140	−7.616	−5.40 (−5.40)
	$H_{3,5}$	−2.380	−1.204	−2.296	−2.296	ca. 0
	H_4	−27.27	−30.69	−26.38	−28.34	−27.42 (−30.19)
ρ_π[b]	1	0.321	0.340	0.323	0.324	
	2,6	0.087	0.088	0.086	0.086	
	3,5	0.017	−0.003	0.017	0.015	
	4	0.363	0.397	0.366	0.369	
p-xylene$^+$						
^{1}H-hf	CH_3	56.95	50.51	51.10	51.18	53.08 (51.63)
	$H_{2,3,5,6}$	−5.152	−4.844	−4.816	−5.068	−10.47 (−9.04)
ρ_π	1,4	0.309	0.340	0.315	0.317	
	2,3,5,6	0.054	0.048	0.056	0.055	
o-xylene$^+$						
^{1}H-hf	CH_3	47.68	43.98	42.59	42.63	(37.36)
	$H_{3,6}$	2.025	4.034	2.036	2.360	
	$H_{5,4}$	−15.41	−17.28	−14.80	−15.87	(−15.53)
ρ_π	1,2	0.276	0.299	0.280	0.282	
	3,6	−0.050	−0.077	−0.051	−0.054	
	5,4	0.203	0.218	0.205	0.206	
m-xylene$^+$						
^{1}H-hf	CH_3	39.91	36.01	35.87	35.85	34.67
	H_2	1.158	2.749	1.225	1.435	
	$H_{4,6}$	−23.36	−26.07	−22.26	−23.89	
	H_5	3.629	6.288	3.468	3.694	
ρ_π	1,3	0.183	0.193	0.189	0.190	
	2	−0.039	−0.060	−0.041	−0.043	
	4,6	0.307	0.330	0.307	0.309	
	5	−0.069	−0.105	−0.069	−0.074	

[a] All calculations were performed by using 6-31++G(d,p) basis sets. [b] ρ_π stands for π-electron spin densities on the ring carbons. [c] Experimental values in CF_3CCl_3 and $CFCl_3$ (in parentheses) are shown.

have smaller spin density than the spin density in toluene cations. However, the spin densities on the four equivalent ring carbons have averaged values of the ring carbons of toluene cations. The spin densities on the α-carbons in *o*- and *m*-xylene cations with the $^2B_{1g}$ type of ground state were smaller than the spin density of the $^2B_{2g}$ type of state as expected by a simple prediction.

Theoretical isotropic ^{1}H-hyperfine coupling constants for the series of methyl-substituted benzene cations are shown along with their spin density on the carbons in Table 3. In each cation, the theoretical hyperfine coupling constants are in good agreement with the experimental ones, although the hyperfine coupling constants of methyl protons in BLYP are slightly overestimated. As was seen in the experimental values, the hyperfine coupling constants of methyl protons decreased in the order of toluene, *p*-xylene, *o*-xylene, and *m*-xylene. Since the C−CH_3 bond lengths are almost the same in all cations, the decrease of hyperfine coupling constant is affected by the decreasing π-electron spin densities of α-carbons.

(iii) Dipolar ^{1}H Hyperfine Couplings. The anisotropic hyperfine couplings of the ring protons, H_4 for toluene and $H_{2,3,5,6}$ for *p*-xylene, was observed in the ENDOR spectra of the toluene and *p*-xylene cations. In the case of *p*-xylene, one of the principal hyperfine components could be hidden in the instrumental artifact which can give small error in the estimation of dipolar hyperfine coupling constants. In order to support the assignments of the anisotropic hyperfine transitions for these cations, theoretical calculations for dipolar hyperfine tensors were performed using INDO spin densities based on the optimized geometry by B3LYP/6-31++G(d,p). The results are shown in Table 2 together with the experimental values. The calculated values are in good agreement with the experimental ones. Affected by the spin density on the bonding carbon, the dipolar couplings for *p*-xylene cations are much smaller than the dipolar couplings for toluene cation, but still large enough to be detected by ENDOR. The anisotropic hyperfine coupling tensors obtained from ENDOR measurements were in agreement with the results obtained by INDO calculations for the corresponding radical cations. We also carried out calculations of the dipolar tensor for *o*-xylene and *m*-xylene radical cations but the ENDOR transitions of these cations were not clearly assigned. The calculations showed that the dipolar hyperfine coupling is large enough to be observed by ENDOR: $B_x = 11.65$ MHz, $B_y = -2.59$ MHz, and $B_z = -9.06$ MHz for H_4 and H_5 in *o*-xylene and $B_x = 18.18$ MHz, $B_y = -3.29$ MHz, and $B_z = -14.89$ MHz for H_4 and H_6 in *m*-xylene.

5. Conclusions

The hyperfine coupling constants of methyl protons and ring protons for toluene and *p*-xylene radical cations in $CFCl_3$ and CF_3CCl_3 matrices have been accurately determined by ENDOR. The ENDOR studies gave evidence for the anisotropic hyperfine interaction for the para proton in the radical cation of toluene. The dipolar coupling constants obtained from ENDOR measurements are in close agreement with those obtained from INDO spin density calculations. The hyperfine anisotropy obtained for ring protons in the case of *p*-xylene was relatively small due to small spin density on ring protons and the values of dipolar coupling are consistent with theoretical results. From the spin density calculations the methyl-substituted benzenes were classified into two groups: toluene and *p*-xylene are of the $^2B_{2g}$ type, and *o*-xylene and *m*-xylene are of the $^2B_{1g}$ type. The theoretical calculations using DFT strongly supported the experimental results.

Acknowledgment. The present study has been financially supported by NFR (Swedish National Science Research Council), STINT (The Swedish Foundation for International Cooperation in Research and Higher Education), and the Swedish Institute. We acknowledge Dr. N. Benetis and Ms. M. Löfkvist for valuable comments on the manuscript.

References and Notes

(1) Edlund, O.; Kinell, P.-O.; Lund, A.; Shimizu, A. *J. Chem. Phys.* **1967**, *46*, 3679.

(2) Komatsu, T.; Lund, A. *J. Phys. Chem.* **1972**, *76*, 1727.

(3) Kinell, P.-O.; Lund, A.; Shimizu, A. *J. Phys. Chem.* **1969**, *73*, 4175.

(4) Volodin, A.; Bolshov, V. A.; Panov, G. *J. Phys. Chem.* **1994**, *98*, 7548.

(5) Bolshov, V. A.; Volodin, A. M.; Zhidomirov, G. M.; Shubin, A. A.; Bedilo, A. *J. Phys. Chem.* **1994**, *98*, 7551.

(6) Kadam, R. M.; Erickson, R.; Komaguchi, K.; Shiotani, M.; Lund, A. *Chem. Phys. Lett.* **1998**, *290*, 371.

(7) Vérdin, J. C.; Auroux, A.; Bolis, V.; Dejaifve, P.; Naccache, C.; Wirezchowski, P.; Derouhane, E. G.; Nagy, J. B.; Gilson, J.-P.; van Hooff, J. H. C.; van den Berg, J. P.; Wolthuizen, J. *J. Catal.* **1979**, *59*, 248.

(8) Erickson, R.; Lund, A.; Lindgren, M. *Chem. Phys.* **1995**, *193*, 89.

(9) Erickson, R.; Benetis, N. P.; Lund, A.; Lindgren, M. *J. Phys. Chem.* **1997**, *101*, 2390.

(10) Erickson, R.; Lindgren, M.; Lund, A.; Sjöqvist, L. *Colloids Surf. A* **1993**, *72*, 207.

(11) Greson, F.; Qin, X.-Z. *Chem. Phys. Lett*. **1988**, *153*, 546.

(12) Iwasaki, M.; Toriyama, K., Nunoma, K. *J. Chem. Soc., Chem. Commun.* **1983**, 320.

(13) Tuttle; T. R.; Weissman; S. I.; Jr. *J. Am. Chem. Soc*. **1958**, *80*, 5342.

(14) Stevenson, C. D.; Wagner, E. P.; Reiter, R. C. *J. Phys. Chem.* **1993**, *97*, 10587.

(15) Nagai, S.; Ohnishi, S.; Nitta, I. *Bull. Chem. Soc. Jpn.* **1971**, *44*, 1230.

(16) Tabata, M.; Lund, A. *Chem. Phys.* **1983**, *78*, 379.

(17) Symons, M. C. R.; Harris, L. *J. Chem. Res. (S)* **1982**, 268.

(18) Komatsu, T.; Lund, A. *J. Phys. Chem.* **1972**, *76*, 1721.

(19) Frisch, M. J.; Trucks, G. W.; Schlegel, H. B.; Gill, P. M. W.; Johnson, B. G.; Robb, M. A.; Cheeseman, J. R.; Keith, T.; Petersson, G. A.; Montgomery, J. A.; Raghavachari, R.; Al-Laham, M. A.; Zakrzewski, V. G.; Ortiz, J. V.; Foresman, J. B.; Cioslowski, J.; Stefanov, B. B.; Nanayakkara, A.; Challacombe, M.; Peng, C. Y.; Ayala, P. Y.; Chen, W.; Wong, M. W.; Andres, J. L.; Replogle, E. S.; Gomperts, R.; Martin, R. L.; Fox, D. J.; Binkley, J. S.; Defrees, D. J.; Baker, J.; Stewart, J. P.; Head-Gordon, M.; Gonzalez, C.; Pople, J. A. *Gaussian 94*, Revision C.3; Gaussian, Inc.: Pittsburgh, PA, 1995.

(20) Edlund, O.; Lund, A.; Shiotani, M.; Sohma, J.; Thuomas, K.-Å. *Mol. Phys.* **1976**, *32*, 49.

(21) Whiffen, D. H. *Mol. Phys.* **1966**, *10*, 595.

(22) Toriyama, K.; Numome, K.; Iwasaki, M. *J. Chem. Phys.* **1976**, *64*, 348.

(23) Schweiger, A.; Günthard, Hs. H. *Chem. Phys.* **1982**, *70*, 1.

(24) Hasegawa, A.; Itagaki, Y.; Shiotani, M. *J. Chem. Soc., Perkin Trans. 2* **1997**, 1625.

(25) Huang, M.-B.; Lunell, S. *J. Chem. Phys.* **1990**, *92(10)*, 6081.

(26) Chandra, H.; Symons, M. C. R.; Hasegawa, A. *J. Chem. Soc., Faraday Trans. 1*, **1987**, *83*, 759.